ELSEVIER

International Journal of Mass Spectrometry 219 (2002) 295–303

International Journal of Mass Spectrometry

www.elsevier.com/locate/ijms

1,3-H-shift pathways in $C_2H_4O^{\bullet+}$ and C_2H_4O

Charles E. Hudson, David J. McAdoo*

Marine Biomedical Institute, University of Texas Medical Branch, 301 University Boulevard, Galveston, TX 77555-1043, USA

Received 26 December 2001; accepted 20 May 2002

Abstract

The 1,3-H-shifts that would interconvert the C_2H_4O aldehyde and enol isomers and the corresponding radical cations are characterized by theory to examine further the influence of Woodward–Hoffmann (WH) orbital symmetry constraints on those reactions. Reaction pathways are traced using intrinsic reaction coordinate methods. The interconversion of the ions avoids WH restraints by rotation of the methylene such that the transition state is neither suprafacial nor antarafacial. However, the neutrals appear to interconvert through a "forbidden" suprafacial transition state with an associated avoided curve crossing such that electronic ground state reactants give products in their ground electronic state. This is the first violation of WH constraints found in a 1,3-H-shift. Present results together with previous work demonstrates that 1,3-H-shifts across double bonds can be antarafacial, suprafacial or in between. (Int J Mass Spectrom 219 (2002) 295–303)

Keywords: C_2H_4O; 1,3-H-shifts; Orbital symmetry; Ab initio; Woodward–Hoffmann

1. Introduction

We use theory to expand our knowledge of 1,3-H-shifts across double bonds, an incompletely explored area. A sigmatropic 1,3-H-shift across double bonds would violate Woodward–Hoffmann (WH) conservation of orbital symmetry if suprafacial, and an allowed antarafacial transition states for such a shift would be substantially strained [1], making it hard to predict the nature of the transition state such reactions utilize when they do occur. Theoretical evidence for both antarafacial and suprafacial 1,3-H-shifts across double bonds has been presented over the past 25 years [2–10]. To date all of the latter reactions are essentially two consecutive 1,2-shifts rather than 1,3-shifts [2–4], so they are not really forbidden, and there is good evidence for antarafacial 1,3-H-shifts only for propene [4–6], ionized propene [7,9] and CH_3O^+=$CHCH_3$ [10]. Although the isomerization of propene may not actually occur because of competition from the loss of $H^\bullet$ [4], unimolecular 1,3-H-shifts across double bonds do take place in several radical cations [11–17] and in enolate anions [18,19]. Such reactions typically have high critical energies around 210 kJ mol^{-1} [14,20,21].

In the transition state for the degenerate isomerization of the acetone enolate ion semiempirical theory oriented the methylenes perpendicular to the skeletal plane [19], a geometry at which π-bonding would be completely eliminated; this revealed an apparent mechanism for avoiding Woodward–Hoffman constraints. However, we found recently by ab initio theory that the methylene hydrogens are asymmetric to the skeletal plane at that transition state such that the

* Corresponding author. E-mail: djmcadoo@utmb.edu

1387-3806/02/$ – see front matter © 2002 Published by Elsevier Science B.V.
PII S1387-3806(02)00730-3

reaction is actually antarafacial (Hudson and McAdoo, unpublished observations) like the isomerizations of propene and the propene ion. Ironically however, we have also found that elimination of π-bonding by methylene rotation does occur in the 1,3-H-shift $CH_3{}^+O{=}CH_2 \rightarrow CH_2{=}O^+CH_3$, that reaction passing through a transition state with the hydrogens in each methylene placed symmetrically on opposite sides of a plane containing the heavy atoms and the migrating hydrogen [10]. The planar symmetry of this transition state places the reaction at the boundary between being suprafacial and being antarafacial, demonstrating that going through such a geometry is after all a feasible mechanism for avoiding WH-restraints.

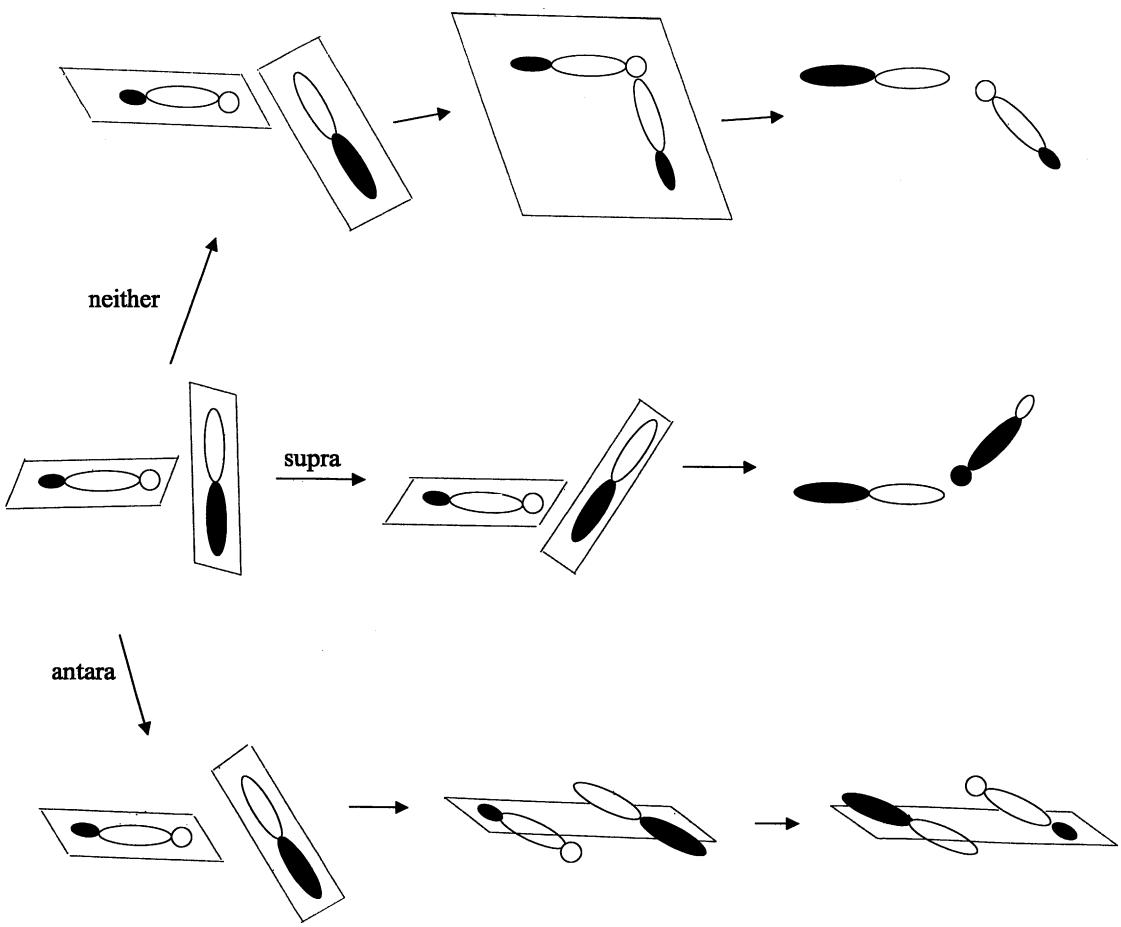

Fig. 1. Diagrams illustrating the orbital transformations along possible pathways for 1,3-H-shifts. Light lobes represent portions of the orbital with a phase of one sign and the dark lobes the opposite phase. Each parallelogram represents a plane such that all lobes completely enclosed within it are in that plane. The diagram of the starting point of the reactions depicts lobes of the OH bond and the π-orbital on the methylene carbon in the enol isomers of C_2H_4O and $C_2H_4O^{\bullet+}$. The π-lobes are perpendicular to the planes of those structures. The upper pathway represents rotation about the π-bond such that the methylene becomes symmetric relative to the skeletal plane, completely breaking off π-bonding. H-transfer occurs in the skeletal plane without the H crossing that plane, so the reaction is neither suprafacial nor antarafacial. In the middle reaction, the H is transferred from the positive lobe of the orbital constituting the HO bond to the negative lobe of the π-bond. In this case the H does not cross the skeletal plane, so the reaction is suprafacial. In the bottom pathway, H transfers from the positive lobe of the O–H orbital to the positive lobe of the π-orbital on the methylene carbon at the same time crossing the skeletal plane. This pathway is antarafacial.

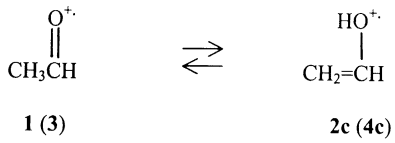

Scheme 1.

Orbital transformations during these different types of reaction pathways for 1,3-shifts are illustrated in Fig. 1. The variety of transition states reported for 1,3-H-shifts across double bonds demonstrates that there is not yet a general picture of the pathways by which those transfers may take place.

It is clear that 1,3-H-shifts convert some enol radical cations to keto isomers in the gas phase [11–17], so we utilized theory to characterize 1,3-H-shifts across double bonds (Scheme 1) that would interconvert the aldehyde and enol isomers of $C_2H_4O^{\bullet+}$ radical cations (**1** and **2**). We also characterized the corresponding reaction in C_2H_4O neutrals (**3** and **4**) to compare reactions of open and closed shell species. Together with propene, these are the simplest systems able in principle to undergo the reaction of interest. Several groups have characterized the stationary points, although not the complete reaction coordinates, of these reactions [2,3,17,22–25]. It should be noted that the 1,3-H-shift **1** $\rightleftarrows$ **2** does not occur experimentally due to competition from more energetically favored $H^{\bullet}$ loss [17,25], and that the interconversion of the neutrals in solution involves base or acid catalysis rather than being unimolecular.

2. Theory

All calculations were performed using the Gaussian 94 or the Gaussian 98W packages of programs [26,27]. Geometries were obtained by B3LYP/6-31G(d,p) hybrid functional and QCISD/6-31G(d,p) ab initio theories. Ab initio {QCISD(T)/6-311G(d,p), QCISD(T) + ΔE (ΔE = QCISD/6-311+G(2df,2pd) − QCISD/6-311G(d,p)) and QCISD(T)/6-311+G(3df,2p)} and {B3LYP/6-311G(d,p)} theories were used to obtain the energies of stationary points. The reaction trajectories were determined by intrinsic reaction coordinate (IRC) methods [28,29] together with B3LYP/6-31G(d) theory. Interactions between atoms were classified as bonding or antibonding based on the orbital coefficients at each atom, phases of like sign between adjacent atoms being taken as bonding and adjacent phases of opposite sign being taken as antibonding. Orbital descriptions were obtained by QCISD/6-31G(d,p) theory. Zero point energies were obtained by multiplying those derived from frequencies produced by B3LYP/6-31G(d,p) theory by the scaling factor 0.9806 [30]. Atoms in molecules (AIM) theory using QCI density was used to obtain covalent bond orders [31].

3. Stationary point characteristics

The geometries of the stationary points of the reactions of interest are given in Figs. 2 and 3. The enol species are depicted in their *cis* geometries, the configurations which would participate in the 1,3-H-shifts. Energies obtained at several levels of theory are given in Tables 1 and 2. The results of these calculations are similar to ones obtained previously by others for these systems where comparisons can be made [22–25]. Our TS(**1** $\rightleftarrows$ **2c**) is 212 kJ mol^{-1} above *trans*-**2**, in good agreement with a value of 215 kJ mol^{-1} obtained by Bertrand and Bouchoux [25]. Our best energy for *cis*-**4** relative to **3**, 46.4 kJ mol^{-1}, agrees very well with a recent value of 47 kJ mol^{-1} reported by Radom and coworkers, as does our value for TS(**3** $\rightleftarrows$ **4c**), 284 kJ mol^{-1}, vs. their value of 282 kJ mol^{-1} [23]. For *cis*-**4** our QCISD/6-31G(d,p) bond lengths and angles are within 0.003 Å and 1° of experimental values [22] and within 0.005 Å and 1.3° of previous results from theory [23]. Potential diagrams depicting the reaction coordinates for the two reactions studied are given in Fig. 4.

4. Interconversion of the radical cations 1 and 2

Although the stationary points on the surface for **1** $\rightleftarrows$ **2** were previously characterized by theory [17,25],

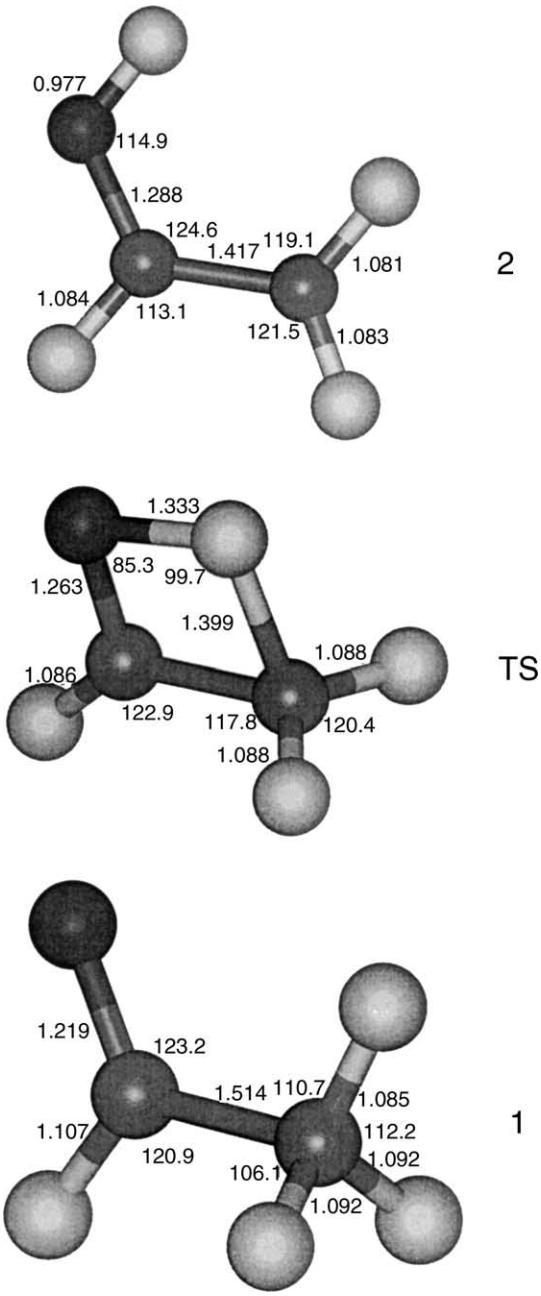

Fig. 2. QCISD/6-31G(d,p) geometries for CH_2=$CHOH^{\bullet+}$ (top), $CH_3CHO^{\bullet+}$ (bottom) and the transition state interconverting them (middle).

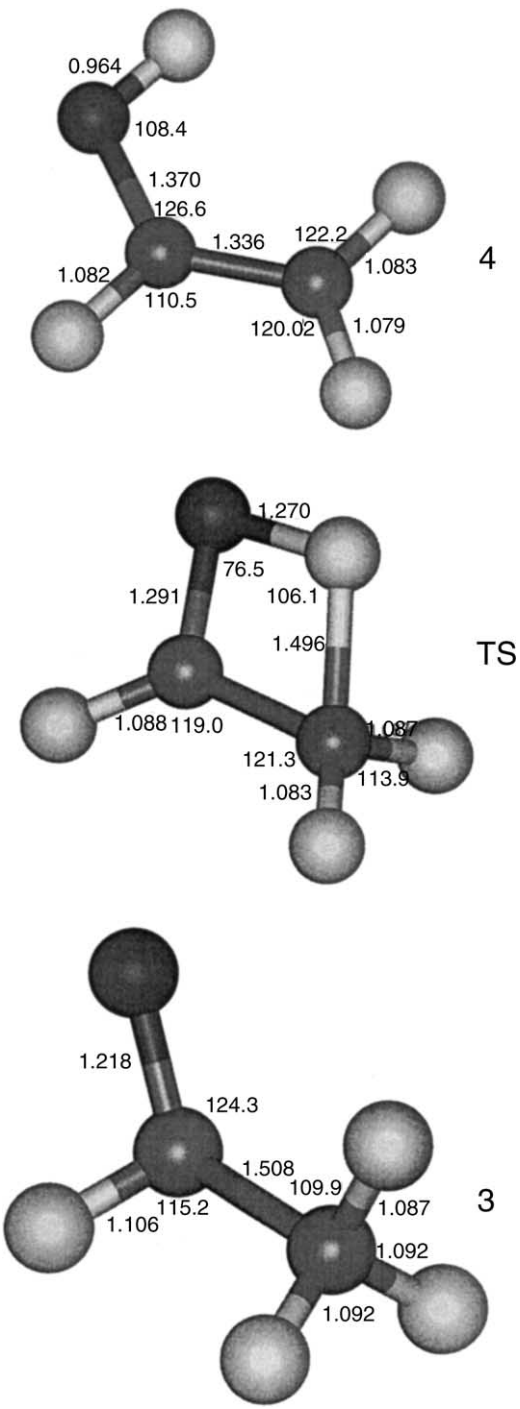

Fig. 3. QCISD/6-31G(d,p) geometries for CH_2=$CHOH$ (top), CH_3CHO (bottom) and the transition state interconverting them (middle).

Table 1
Theoretical energies (Hartrees) of stationary points

Species	B3LYP/6-311G(d,p)// B3LYP/6-31G(d,p)	QCISD(T)6-311G(d,p)// QCISD/6-31G(d,p)	QCISD(T) + ΔE[a]	QCISD(T)/6-311+G (3df,2p)//QCISD/6-31G(d,p)
$CH_3CHO^{\bullet+}$ (**1**)	−153.506855	−153.1216030	−153.202389	−153.208951
CH_2=$CHOH^{\bullet+}$ (**2c**)	−153.526521	−153.1381200	−153.223210	−153.228602
CH_2=$CHOH^{\bullet+}$ (**2t**)	−153.530163	−153.1412660	−153.226189	−153.231550
TS(**1**⇄**2c**)	−153.441229	−153.055372	−153.139951	−153.143942
CH_3CHO (**3**)	−153.876778	−153.4859540	−153.576284	−153.583544
CH_2=CHOH (**4c**)	−153.859657	−153.4662830	−153.560772	−153.566796
CH_2=CHOH (**4t**)	−153.856685	−153.4632990	−153.558705	−153.564834
TS(**3**⇄**4c**)	−153.765928	−153.3706610	−153.463598	−153.470376

[a] ΔE = (QCISD/6-311+G(2df,2pd) − QCISD/6-311G(d,p)).

the pathways connecting them were not. Fig. 5 gives dihedral angles involving H_t or a methylene hydrogen as a function of CH_t distance along the reaction coordinate obtained for **1** ⇄ **2** using B3LYP/6-31G(d) IRC computations, results that can be used to classify the reactions as antarafacial, suprafacial or in between. At TS(**1** ⇄ **2**), H_t is slightly closer to O than to C (1.333 Å vs. 1.399 Å); the similarity of these distances places the transition state about halfway between the reactant and the product. The covalent bond orders for the interactions of H_t with O, C1 and C2 were 0.4295, 0.0470 and 0.4133 in this transition state. This demonstrates little interaction between H_t and C1 during the shift, establishing that this is a 1,3-H-transfer rather than two consecutive 1,2-shifts.

The H_tCCO dihedral angle remains 0° during most of the course of H-migration and then deviates to a maximum of only 0.7° and then declines back to 0° over about the last 0.1 Å of the transfer of H_t in forming **2**. The other two methyl hydrogens move together toward the skeletal plane at the start of isomerization from **1** and maintain symmetry to the plane within at most 1° until about the last 0.1 Å of the H_t transfer to form **2**. The squeezing of CH_2 takes about one-third of the activation energy for the reaction, the remainder being needed to move H_t from C to O. Over the last 0.1 Å of **1** → **2**, i.e., only very close to the equilibrium geometry of the enol structure **2**, the methylene rotates dramatically to its orientation in **2**. It takes about 75 kJ mol^{-1} to distort **2** from its mini-

Table 2
Theoretical energies (kJ mol^{-1}) of stationary points

Species[a]	B3LYP/ 6-311G(d,p)	QCISD(T)/ 6-311G(d,p)	QCISD(T) + ΔE	QCISD(T)/ 6-311+G(3df,2p)	Experimental[b]
$CH_3CHO^{\bullet+}$ (**1**)	43.7	35.5	46.8	43.7	821, 50
CH_2=$CHOH^{\bullet+}$ (**2c**)	0.0	0.0	0.0	0.0	
CH_2=$CHOH^{\bullet+}$ (**2t**)	−9.3	−8.0	−7.5	−7.4	771[c], 0
TS(**1**⇄**2c**)	206.2	199.6	200.9	204.6	
$CH_3CO^+ + H^{\bullet}$					871, 100
CH_3CHO (**3**)	0.0	0.0	0.0	0.0	−166, 0
CH_2=CHOH (**4c**)	47.4	54.0	43.1	46.4	−114[b], 52
CH_2=CHOH (**4t**)	53.9	60.6	47.3	50.2	
TS(**3**⇄**4c**)	277.9	289.6	282.8	284.0	
$CH_3CO^{\bullet} + H^{\bullet}$					194, 360

[a] Geometries were optimized at levels of theory indicated in column headings in Table 1.
[b] [39].
[c] [40].

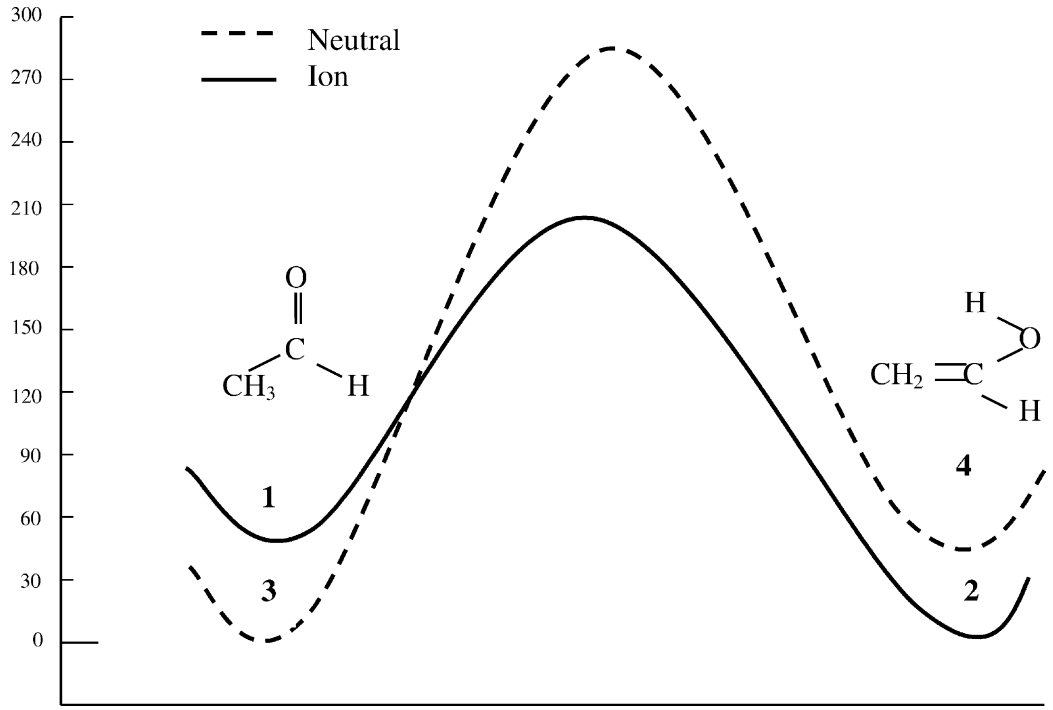

Fig. 4. Potential diagrams for the interconversion of aldehyde and enol isomers of $C_2H_4O^{\bullet+}$ and $C_2H_4O^{\bullet+}$ isomers based on QCISD(T)/6-311+G(3df,2p) energies.

mum energy planar geometry to a configuration with the angles between the CH_2 hydrogens and the skeletal plane differing by only 1°; during this motion the CH_t distance decreases by only 0.2 Å and the OH_t length increases by only 0.01 Å. Thus, CH_2 rotation occurs essentially separately from the H-transfer, and π-bonding is largely broken off before the H-transfer in **2** ⇄ **1** is initiated. There is no crossing of the CCO plane by the migrating H_t, so this reaction is suprafacial to the extent that it can be classified on the basis of a 0.7° deviation of H_t from planarity far from the transition state. However, because π-bonding is completely eliminated over most of the course of this reaction, Woodward–Hoffmann constraints are effectively evaded. The symmetry of the methylene to the skeletal plane at the transition state for this reaction is very much like that found for the degenerate isomerization of $CH_3{}^+O{=}CH_2$. Thus, as in $CH_3{}^+O{=}CH_2$, interconversion of **1** and **2** avoids W–H constraints by minimally avoiding a suprafacial transition state without becoming antarafacial. Therefore, this type of pathway can occur in both open and closed shell reactants.

Woodward–Hoffman restraints might direct the products of 1,3-H-shifts to electronically-excited products through suprafacial transition states [1,14,32–34]. However, the first electronically excited doublet state of **1**, the A state, is about 232 kJ mol^{-1} above the vibrationally cold ground state [33], substantially exceeding the 161 kJ mol^{-1} required for **1** → **2**. Even though there might be a slightly lower quartet state, reaction to it would be unlikely because it would require inversion of the spin of an electron. Thus, this reaction probably does not produce electronically excited products by isomerization from ground states, or vice versa. This is as would be expected for the transition state with the methylene perpendicular to the skeletal plane.

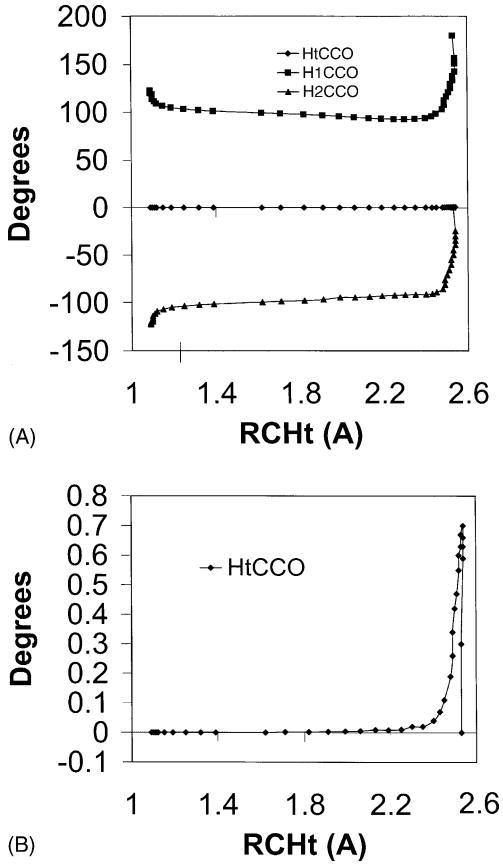

Fig. 5. (A) Changes in dihedral angles as a function of CH_t distance during the interconversion of CH_2=$CHOH^{\bullet+}$ and $CH_3CHO^{\bullet+}$. Results were obtained by IRC calculations utilizing B3LYP/6-31G(d) theory. The vertical line on the *X*-axis at 1.26 Å depicts the location of the transition state. (B) The change in the COH_tC dihedral angle on an expanded *Y*-axis.

5. Interconversion of the neutral C_2H_4O isomers

We examined the interconversion of **3** and **4** to see if in the course of those isomerizations there might be differences in the rotation about the CC π-bond depending on whether it contains one or two electrons. Relative to the distances in TS(**1** ⇄ **2**), in TS(**3** ⇄ **4**), H_t is slightly closer to O and farther from C (the OH distance = 1.270 Å and CH distance = 1.496 Å). This is as would be expected based on Hammond's postulate [35], given that **3** is lower in energy than **4**, and **1** is higher in energy than **2**. Covalent bond orders

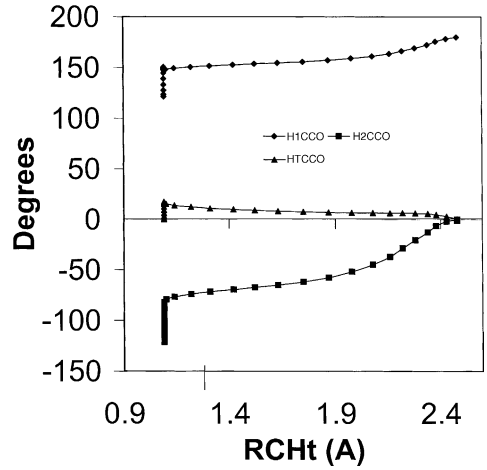

Fig. 6. Changes in dihedral angles as a function of CH_t distance during the interconversion of CH_2=CHOH and CH_3CHO. The vertical line on the *X*-axis at 1.29 Å depicts the location of the transition state. Results were obtained by IRC calculations with B3LYP/6-31G(d) theory.

between H_t and O, C1 and C2 in TS(**3** ⇄ **4**) derived by AIM analysis were 0.3960, 0.0875 and 0.3708, respectively, demonstrating much less interaction between H_t and C1 than of H_t with O and C2 in the course of the reaction. Thus, TS(**3** ⇄ **4**) is also clearly for a 1,3-H-shift rather than two consecutive 1,2-shifts.

Fig. 6 gives changes in dihedral angles during the interconversion of the neutrals. This pathway differs markedly from that of **1** ⇄ **2** in that **3** ⇄ **4** is initiated by a substantial rotation of the methyl prior to appreciable CH_t lengthening. Near the start of **3** → **4**, as the CH_t bond lengthens from 1.0923 to 1.0930 Å in B3LYP/6-31G(d) theory, i.e., only 0.007 Å, one HCCO dihedral angle for a methylene H rotates by 24.0° and the other by 37.3°. As the reaction continues, the former angle increases slowly to 180° at **4**, while over the same time the latter angle decreases to 0°. The H that moves to the *trans* position rotates 56°, and the angle to the hydrogen that becomes *cis* relative to O changes 119° in the overall course of the reaction. Thus, 45% of the total change of the first angle and 34% of the change of the second occur before appreciable CH_t lengthening occurs. Both of the HCCO dihedral angles change continuously to their

final values throughout the remainder of the transfer of H_t in **3** → **4**. In contrast to H_t remaining within 0.7° of the skeletal plane over the course of **1** ⇄ **2**, H_t moves almost 18° from being in the skeletal plane in **3** ⇄ **4** before it begins to move toward the oxygen. This angle then slowly decreases as CH_t lengthens, and finally drops abruptly from about 6–0° over the last 0.1 Å of that lengthening.

In **1** ⇄ **2** the rotation of CH_2 occurs very close to the enol structure, i.e., only when H_t is completely separated from the carbon from which it departs. In contrast in **3** → **4** much of the rotation occurs very close to the aldehyde minimum and the remainder gradually takes place across the course of H-transfer. In short, the necessary change in geometry is accomplished by a methylene rotation in **1** ⇄ **2** and by a methyl rotation in **3** ⇄ **4**. The difference is probably due to a combination of WH constraints with easier twisting of CH_2 when an electron is missing from the double bond vs. easier rotation about a single bond. The 60 kJ mol^{-1} associated with CH_3 rotation in the initiation of H-transfer from **3** is also surprising. This energy is not required simply to rotate CH_3, as the barrier to methyl rotation in **3** is only 4.1 kJ mol^{-1} (from B3LYP/6-311G(d,p) theory).

Despite substantial searching, we found no antarafacial transition states or pathways for **3** ⇄ **4** involving two consecutive 1,2-H_t-shifts. This contrasts with early work on **3** → **4** using low levels of theory [2,3], which found a "suprafacial" pathway in which H-transfer occurred in essentially two consecutive 1,2-H-shifts and a favored "antarafacial" pathway in which H was transferred by a direct 1,3-shift. At no time in **3** ⇄ **4** does the H cross the skeletal plane, so the reaction is suprafacial based on the criterion that reactions in which H_t does not cross the skeletal plane are suprafacial. To our knowledge, all previously characterized 1,3-H-shifts are either antarafacial [4–6,7,9] or neither antarafacial nor suprafacial [10].

Our critical energy from theory for **3** → **4** (284 kJ mol^{-1}) is lower than the experimental heat of reaction for **4** → $CH_3CO^{\bullet} + H^{\bullet}$ (360 kJ mol^{-1}), suggesting that **4** ⇄ **3** can occur unimolecularly at high internal energies. This is supported by **4** ⇄ **3** being the lowest energy reaction for **3** and **4** found in a comprehensive theoretical study of the C_2H_4O potential surface [23].

The first singlet electronically excited state of **3** is at 356 kJ mol^{-1} [36,37] and the first electronic triplet is at 326 kJ mol^{-1} [37], both well above the 284 kJ mol^{-1} required for **3** → **4**. Thus, this reaction does not form electronically excited products from ground state reactants, despite WH-predictions that excited products would form via suprafacial transition states. *Therefore*, **3** → **4** *appears to provide the first clear suprafacial violation of the Woodward–Hoffmann constraints in a 1,3-H-shift*.

If suprafacial **3** → **4** is indeed WH forbidden, the H would be attempting to transfer between regions of opposite phase in the pertinent orbitals. In the transition state for interconverting **3** and **4**, consideration of the phases of the three highest occupied orbitals encompassing C2, H_t and O (these orbitals have larger coefficients for the H_t's functions associated with H_t than do the remaining orbitals and therefore are the ones representing the bonding to H_t) indicates a bonding interaction between C2 and H_t and an antibonding interaction between H_t and O. This is in accord with the WH prediction that this reaction should not occur by a suprafacial pathway since the transition state energy is too low to allow formation of products in an excited state and reaction through the transition state located requires an avoided curve crossing in order to circumvent the WH constraints.

6. Summary

Interconversion of ions **1** and **2** avoids WH constraints by taking a path almost exactly on the boundary between being suprafacial and antarafacial. Unimolecular interconversion of the **3** and **4** appears to go by a WH forbidden pathway because the reaction path is suprafacial and because the orbitals encompassing C2, H_t and O at that transition state are primarily bonding between C2 and H_t, but antibonding between H_t and O. Thus, in this reaction a curve crossing appears to be avoided rather than

an electronically excited state being produced. This appears to be the first identification, at least in theory, of a WH forbidden, suprafacial 1,3-H-shift, although symmetry forbidden, 1-3-shifts of carbon may occur [38]. Present results in combination with previous work demonstrates that sigmatropic 1,3-H-shifts can be antarafacial, suprafacial, or in between.

Acknowledgements

We are grateful to Xia Thomas Chen for assistance with computations and preparing figures.

References

[1] R.B. Woodward, R. Hoffmann, Angew. Chem. 8 (1969) 781.
[2] W.J. Bouma, D. Poppinger, L. Radom, J. Am. Chem. Soc. 99 (1977) 6443.
[3] W.R. Rodwell, W.J. Bouma, L. Radom, Int. J. Quantum Chem. 18 (1980) 107.
[4] F. Bernardi, M.A. Robb, B. Schlegal, G. Tonachini, J. Am. Chem. Soc. 106 (1984) 1198.
[5] G.J.M. Dormans, H.M. Buck, J. Mol. Struct. 136 (1986) 121.
[6] K.N. Houk, Y. Li, J.D. Evanseck, Angew. Chem. Int. Ed. Eng. 31 (1992) 682.
[7] T. Clark, J. Am. Chem. Soc. 109 (1987) 6838.
[8] M.T. Nguyen, W.D. Weringa, T.-K. Ha, J. Phys. Chem. 93 (1989) 7956.
[9] M.T. Nguyen, L. Landuyt, L.G. Vanquickenborne, Chem. Phys. Lett. 182 (1991) 225.
[10] C.E. Hudson, D.J. McAdoo, J. Am. Soc. Mass Spectrom. 9 (1998) 130.
[11] F.W. McLafferty, D.J. McAdoo, J.S. Smith, R. Kornfeld, J. Am. Chem. Soc. 93 (1971) 3720.
[12] L.L. Griffin, D.J. McAdoo, J. Phys. Chem. 83 (1979) 1142.
[13] N. Heinrich, H. Schwarz, J. Am. Chem. Soc. 79 (1987) 295.
[14] N. Heinrich, F. Louage, C. Lifshitz, H. Schwarz, J. Am. Chem. Soc. 110 (1988) 8183.
[15] C. Lifshitz, J. Phys. Chem. 87 (1983) 2304.
[16] D.J. McAdoo, Mass Spectrom. Rev. 19 (2000) 38.
[17] Y. Apeloig, M. Karni, B. Ciommer, G. Depke, G. Frenking, S. Meyn, J. Schmidt, H. Schwarz, Int. J. Mass Spectrom. Ion Process. 59 (1984) 21.
[18] R.N. Hayes, J.C. Sheldon, J.H. Bowie, Int. J. Mass Spectrom. Ion Process. 71 (1986) 233.
[19] K.A. Sannes, J.I. Brauman, J. Am. Chem. Soc. 117 (1995) 10088.
[20] C. Lifshitz, P. Berger, E. Tzidony, Chem. Phys. Lett. 95 (1982) 109.
[21] M. Hofmann, H.F. Schaefer III, J. Phys. Chem. A 103 (1999) 8895.
[22] B.J. Smith, L. Radom, J. Am. Chem. Soc. 112 (1990) 7525.
[23] B.J. Smith, M.T. Nguyen, W.J. Bouma, L. Radom, J. Am. Chem. Soc. 113 (1991) 6452.
[24] F. Turecek, C.J. Cramer, J. Am. Chem. Soc. 117 (1995) 12243.
[25] W. Bertrand, G. Bouchoux, Rapid Commun. Mass Spectrom. 12 (1998) 1697.
[26] M.J. Frisch, G.W. Trucks, H.B. Schlegel, P.M.W. Gill, B.G. Johnson, M.A. Robb, J.R. Cheeseman, T. Keith, G.A. Petersson, J.A. Montgomery, K. Raghavachari, M.A. Al-Laham, V.G. Zakrzewski, J.V. Ortiz, J.B. Foresman, J. Cioslowski, B.B. Stefanov, A. Nanayakkara, M. Challacombe, C.Y. Peng, P.Y. Ayala, W. Chen, M.W. Wong, J.L. Andres, E.S. Replogle, R. Gomperts, R.L. Martin, D.J. Fox, J.S. Binkley, D.J. Defrees, J. Baker, J.P. Stewart, M. Head-Gordon, C. Gonzalez, J.A. Pople, GAUSSIAN 94; Revision E.2, Gaussian, Inc., Pittsburgh, PA, 1995.
[27] M.J. Frisch, G.W. Trucks, H.B. Schlegel, G.E. Scuseria, M.A. Robb, J.R. Cheeseman, V.G. Zakrzewski, J.A. Montgomery Jr., R.E. Stratmann, J.C. Burant, S. Dapprich, J.M. Millam, A.D. Daniels, K.N. Kudin, M.C. Strain, O. Farkus, J. Tomasi, V. Barone, M. Cossi, R. Cammi, B. Mennucci, C. Pomelli, C. Adamo, S. Clifford, J. Ochterski, G.A. Petersson, P.Y. Ayala, Q. Cui, K. Morokuma, D.K. Malick, A.D. Rabuck, K. Raghavachari, J.B. Foresman, J. Cioslowski, J.V. Ortiz, A.G. Baboul, B.B. Stefanov, G. Liu, A. Liashenko, P. Piskorz, I. Komaromi, R. Gomperts, R.L. Martin, D.J. Fox, T. Keith, M.A. Al-Laham, C.Y. Peng, A. Nanayakkara, M. Challacombe, P.M.W. Gill, B. Johnson, W.Chen, M.W. Wong, J.L. Andres, C. Gonzalez, M. Head-Gordon, E.S. Replogle and J.A. Pople, Gaussian, Inc., Pittsburgh, PA, 1998.
[28] C. Gonzalez, H.B. Schlegel, J. Chem. Phys. 90 (1989) 2154.
[29] C. Gonzalez, H.B. Schlegel, J. Phys. Chem. 94 (1990) 5523.
[30] A.P. Scott, L. Radom, J. Phys. Chem. 100 (1996) 16502.
[31] R.F.W. Bader, Atoms in Molecules: A Quantum Theory, Clarendon Press, Oxford, 1990.
[32] F. Turecek, F.W. McLafferty, J. Am. Chem. Soc. 106 (1984) 2525.
[33] R. Bombach, J.-P. Stadelmann, J. Vogt, Chem. Phys. 60 (1981) 293.
[34] R. Zhao, R. Tosh, A. Shukla, J. Futrell, Int. J. Mass Spectrom. Ion Process. 167/168 (1997) 317.
[35] G.S. Hammond, J. Am. Chem. Soc. 77 (1955) 334.
[36] H.-T. Kim, S.L. Anderson, J. Chem. Phys. 114 (2001) 3018.
[37] M. Noble, E.K.C. Lee, J. Chem. Phys. 81 (1984) 1362.
[38] J.A. Berson, Acc. Chem. Res. 5 (1972) 406.
[39] S.G. Lias, J.E. Bartmess, J.F. Liebman, J.L. Holmes, R.D. Levin, W.G. Mallard, J. Phys. Chem. Ref. Data 17 (1988) 87, 90, 616.
[40] J.C. Traeger, M. Djordjevic, Eur. Mass Spectrom. 5 (1999) 319.